Case Studies in Engineering Failure Analysis 5–6 (2016) 23–29

Contents lists available at ScienceDirect

Case Studies in Engineering Failure Analysis

journal homepage: www.elsevier.com/locate/csefa

Case study

Fracture failure analysis of 4Cr13 stainless steel linkages in circuit breakers

Wu Wang-ping

School of Mechanical Engineering, Changzhou University, Changzhou City, Jiangsu Province 213164, China

ARTICLE INFO

Article history:
Received 8 October 2015
Received in revised form 4 January 2016
Accepted 13 January 2016
Available online 22 January 2016

Keywords:
Cleavage fracture
Defects
Failure modes
Fracture surfaces

ABSTRACT

In this study, the fracture failure of the 4Cr13 stainless steel linkage components in circuit breakers was studied. The microstructure and morphology of fracture surface were observed by scanning electron microscopy and optical microscopy. A micro-Vickers tester measured the hardness of the components. The tensile strength and strain of the components were determined by a universal testing machine. The results show that fracture failure mode was quasi-cleavage fracture, and some dimples and edges of cleavage were present on the fracture surface. The substandard sample exhibited higher hardness than the standard sample. The high hardness could cause the strong rigidity and less toughness, which was not helpful to bend the samples to form hook structure. The heat treatment influenced the mechanical properties of the 4Cr13 components. With increasing the tempering temperature, the hardness of the component was decreased when the quenching temperature was kept stable.

1. Introduction

4Cr13, a martensite stainless steel, has a high hardenability, good polishing properties, excellent resistance to corrosion and hot oxidation [1]. Due to these excellent properties, 4Cr13 stainless steel can be applied in several important fields, such as precision mechanism, structural automotive application, and petrochemical industry. During manufacturing process, the heat treatment has significant effect on the mechanical properties of 4Cr13 components. The strength and hardness of 4Cr13 components could remarkably increase after quenching and tempering. However, cracks are induced, finally resulting in the fracture failure of the components under overloading condition. Ouyang et al. [2] suggested that 4Cr13 stainless steel was quenched by a CO_2 laser and tempered for 2 h at different temperatures in the range 200 °C to 550 °C, it was found that the transition of wear mechanism was from mild oxidational wear to severe adhesive wear with the increase of normal load or sliding speed.

In this study, some single-phase circuit breakers (voltage 220 V, frequency 50 Hz) did not normally work during installation processing in one workshop. The 1.45In ampere-second characteristic test was disconnected. The schematic diagram of the circuit breaker is shown in Fig. 1. The free linkage 2 was fractured at the position of 90° angle. It was found that 4Cr13 steel linkage was fractured in the circuit breaker. Fracture modes of many steels were ductile, brittle intergranular or transgranular, fatigue fracture, hydrogen-brittleness. The other reason of fracture failure was even the presence of flaws and foreign inclusion. Hou et al. [3] analyzed fracture mechanism of a 30CrMnSiA steel shaft was fatigue fracture resulting from

E-mail address: wwp3.14@163.com.

http://dx.doi.org/10.1016/j.csefa.2016.01.002

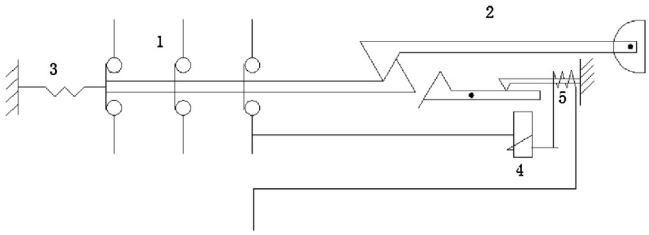

Fig. 1. Schematic diagram of a circuit breaker. 1 – main contact, 2 – free linkage, 3 – main drawspring, 4 – short-circuited release, 5 – overload release.

hydrogen-induced intergranular microcracks. The hydrogen-induced microcracks were caused by abnormal picking during production of the shaft. Sudhakar [4] suggested the failure mechanism of 360 stainless steel nail was predominantly ductile fracture facilitated by the presence of non-metallic inclusion. Pantazopoulos and Papaefthymiou [5] studied that fracture failure of austenitic stainless steel marine propeller shaft was originated from a surface flow where stress raiser acted as fatigue crack initiation. In this case study, the fracture morphology and mechanical properties of 4Cr13 stainless steel linkage components were investigated, and at the same time combined with the heat treatment process for the components, the failure mode of the component was studied.

2. Experimental

Fig. 2 shows the planar geometrical graphs of linkage component. The component was composed of one 90° right angle (the location of failure in Fig. 2c), three R0.1 chamfers and one R0.6 chamfer. The components were manufactured by twice annealings, then twice bendings, subsequently spot welding, quenching and tempering, lastly plating an electroless nickel phosphorus layer. In the first state, the annealing operation of the component was set at a temperature of 880 ± 10 °C and holding 1–2 h, and the subsequent the furnace cooled to room temperature. In the second stage, the upper plate was bonded tightly to down plate by a spot welding process. Subsequently, the annealing operation was again done at a temperature of 700 ± 20 °C and keeping 1–2 h, and then slow cooling to room temperature. The quenching was set at a temperature of 700 ± 20 °C and holding for 25 min, and following oil cooling to room temperature. The tempering temperature was in the range of 510–530 °C.

The microstructure and morphology of fracture surface of linkage components were observed by the optical microscopy and scanning electron microscopy (SEM, FEI CO., Quanta200). The hardness values of the components were tested by a micro-Vickers tester (HV-1000 model) loading 300 g load. The hardness of each sample was averaged after three different points were tested. The tensile strength and strain of the components (size: 10×150 mm) were determined by a universal testing machine (WEW-D model), according to the standard GB/T 228-02.

3. Results and discussion

3.1. Macroscopic

Fig. 3 shows the macrographs of 4Cr13 linkage and the other components. In Fig. 3a and b, the tripping plate was connected with the rod through a square opening with the size of 1.05 mm × 1.8 mm. The size of lateral (X) and longitudinal (Y) directions was 1.0 mm and 1.6 mm, respectively. Therefore, the rod could solidly connect with the tripping plate. During loading condition, there was an elastic force at the position of 90° angle. In Fig. 3c, two solder joints were present on the surface. The spot welding had an influence on the microstructure and mechanical properties of local region near the solder joint on the surface of the component. The component had to be annealed, subsequently. Fig. 3d displays the macrograph of the fractured rod. From the optical micrograph, the fracture surface shows the metallic silver, and a 45° angular along the fracture surface was observed. After the observation and analysis, the fracture failure of the component was brittle fracture in an overloading condition.

3.2. Microscopic

Fig. 4 shows the SEM images of the fracture surface of the component. Fig. 4a illustrates the low magnification image of the fracture surface. The nickel phosphorus layer was plated on the surface of the component. The inner and outer zones of the fracture surface are shown in Fig. 4b and c, respectively. It can be observed that the fracture surface was composed of cleavage terrace, dimple and river pattern. It can be inferred that the fracture failure mode was quasi-cleavage fracture with tore edge.

Fig. 5 displays the optical image of the fracture surface of the component. It can be observed that the grains were fine, and no cracks were present on the fracture surface. After high-temperature tempering, the microstructure of 4Cr13 component

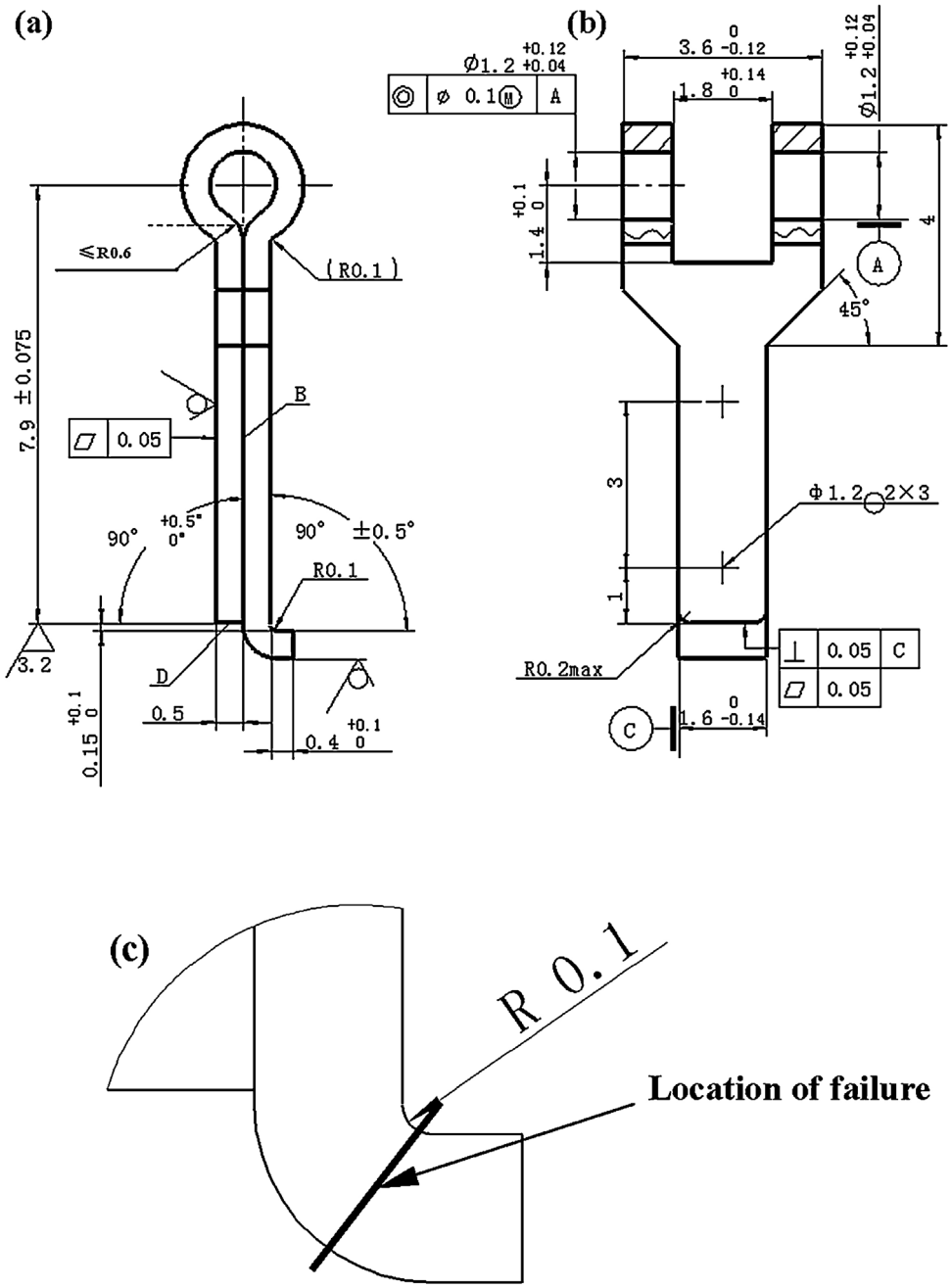

Fig. 2. Planar geometrical graphs of 4Cr13 linkage. (a) Side view, (b) front view and (c) location of failure.

was mainly composed of tempered sorbite, which was a dispersed variety of pearlite with a eutectic mixture of ferrite and cementite. These structures were in line with those of 4Cr13 stainless steel after quenching and tempering.

3.3. Mechanical properties

The hardness values of the substandard and standard products are shown in Table 1. The result shows that the hardness of the substandard product was higher than that of the standard product. The high hardness in crystalline materials could cause the strong rigidity, but resulting in the lack of enough toughness. Therefore, the substandard product was easily fractured under overloading condition. After quenching and tempering, the strength and hardness of 4Cr13 stainless steel increased, but it had severe crack sensitivity. During heat treatment or spot welding, the crack was easily formed. For substandard

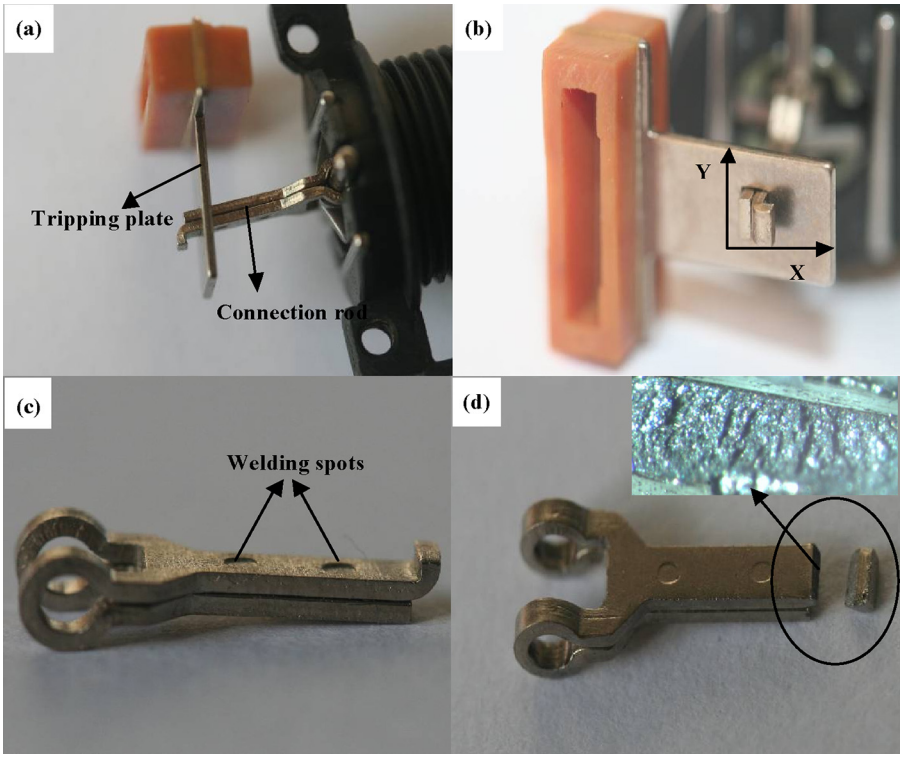

Fig. 3. Macrographs of the linkage and the other components. (a) The tripping plate with positive side and rod, (b) the tripping plate with the other side and rod, (c) linkage and (d) fractured sample.

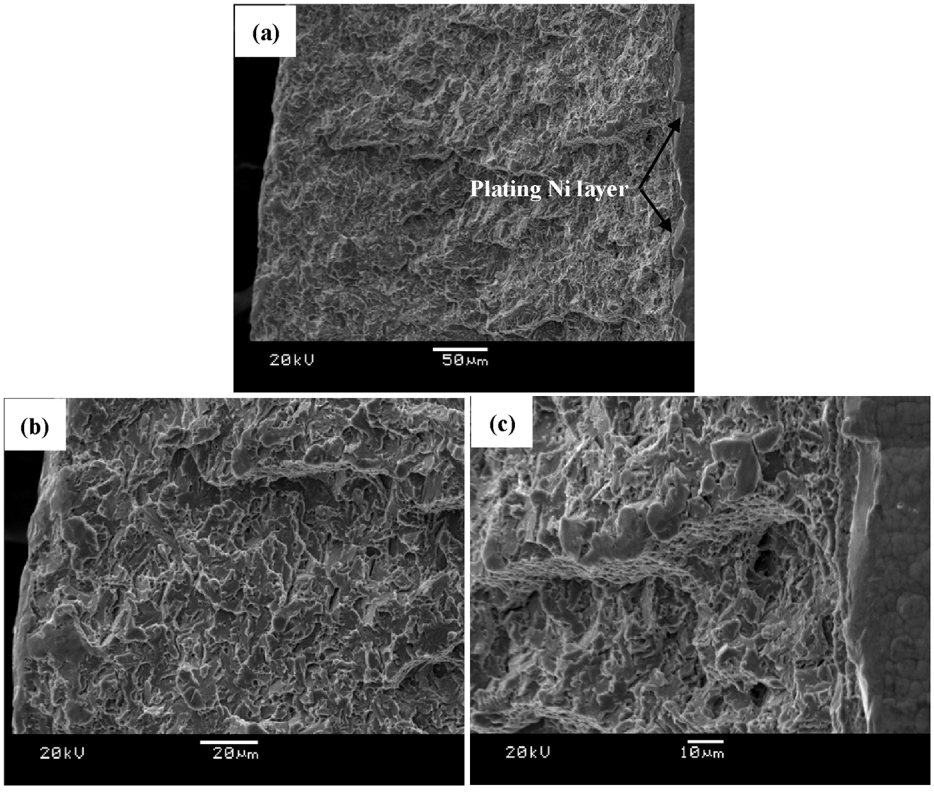

Fig. 4. SEM images of fracture surface of the component. (a) Fracture surface, outer (b) and inner (c) zones at the position of 90° angle

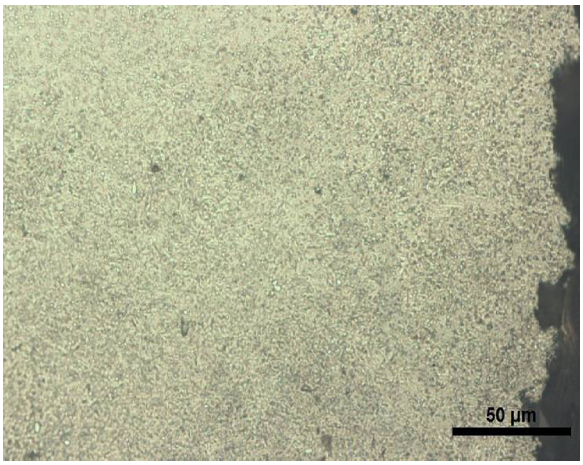

Fig. 5. Optical image of the fracture surface of the rod.

Table 1
Hardness values of the substandard and standard products.

Hardness	Substandard sample	No. 1	No. 2	No. 3
Average hardness (HV0.3)	535.1 ± 10.9	465.9 ± 7.7	493.4 ± 7.3	483.5 ± 9.9
Hardness (HRC)	51.5	47.2	49.1	48.4

Note: Nos. 1–3 samples are the standard samples.

products, there would be quenched residual stress and tempered martensite embrittlement in 4Cr13 stainless steel after heat treatment. The nonuniform distribution of the stress at the position of 90° angle might result in the fracture failure of the rod component in an overloading condition.

The mechanical properties of the 4Cr13 samples are displayed in Table 2. The tempering temperature influenced the mechanical properties of the samples, when the quenching temperature was kept stable. With increasing the tempering temperature, the hardness was decreased. For the sample with a highest hardness of 50.5 $HV_{0.3}$, both fracture position and failure mode were similar to the substandard products. The tensile strength and strain were 1555 MPa and 3.4%, respectively. When the hardness was decreased to 47.1 $HV_{0.3}$, the fracture position and failure mode were unchanged. However, the plastic deformation occurred before the sample started to be fractured. The strain was increased to be 4.2%. When the hardness of the sample was decreased to 40.2 $HV_{0.3}$, the sample was not fractured. These data indicated that the high hardness for metal materials could cause the strong rigidity, but resulting in the decrease of the toughness. While the strength was the controlling property if a component must withstand a specific load, toughness was the limiting property if a component must be capable of absorbing a special quantity of mechanical energy without fracturing [6]. Generally, increasing strength usually leads to decreased toughness.

The SEM images of the fracture surface of the component are shown in Fig. 6. Fig. 6a shows the SEM image of the fracture surface of the standard sample. Fig. 6b displays the SEM image of the fracture surface of the substandard sample. Compared with the fracture surface of the standard sample, the clearage terrace and dimple on the fracture surface of the substandard sample were obvious. It can be inferred that the heat treatment influenced the microstructure of the component. The effect of manufacturing process on the microstructure and mechanical properties of linkage component was further discussed.

Table 2
Mechanical properties of the bending samples and tensile tested samples.

No.	Tempering temperature	Hardness (HRC)	Bending samples	Tensile tested samples
1	510 °C	50.5	F_{max} = 307.2 N, the fracture surface at the position of 90° angle.	σ_b = 1555 MPa, δ = 3.4%, F_{max} = 6939 N
2	525 °C	47.1	F_{max} = 287.2 N, the fracture surface at the position of 90° angle, but plastic deformation occurred before fracture failure.	σ_b = 1364 MPa, δ = 4.2%, F_{max} = 6813 N
3	550 °C	40.2	F_{max} = 231.9 N, the sample was levered at hook.	σ_b = 1175 MPa, δ = 5.2%, F_{max} = 5051 N

Note: Quenching temperature and time were kept stable, 1020 °C × 20 min. Tempering time was 70 min.

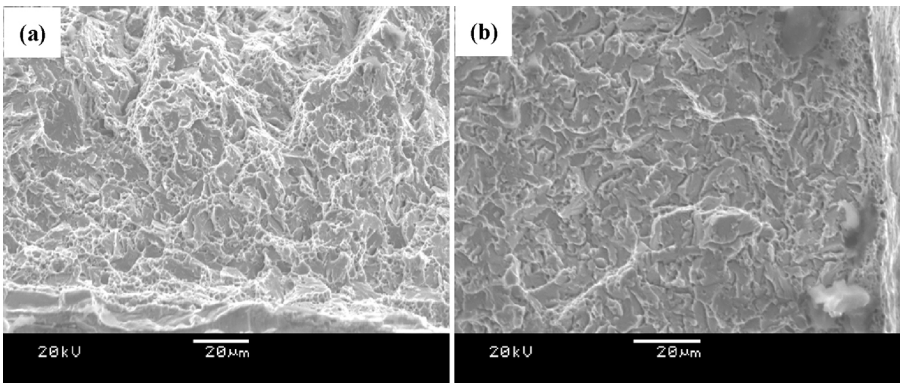

Fig. 6. SEM images of fracture surface of standard (a) and substandard (b) samples.

The manufacturing process is a key factor to make sure the quality of linkage components. In this study, some processes, including annealing, quenching, tempering, bending and electroless plating, were applied to manufacture the linkage components. The rod component was rolled by 4Cr13 strip. The bending direction of the component was perpendicular to the rolling direction, in order to prevent the formation of crack during bending process. At the same time, the deburring, coarse grinding, fine grinding and polishing processes had a significant effect on the mechanical properties of the component.

In the first stage, the softening annealing process was used to improve the plasticity and to prevent fracture failure of the component. After annealing process, no microcracks were found. Subsequently, the upper plate was adhered to the down plate by the spot welding process. During the spot welding, the high temperature would affect the microstructure, mechanical properties and stress status near the solder joint on the surface of the component. After the spot welding, the hardness was increased, but the plasticity was decreased. Therefore, in the second stage, the component had to be annealed before the component was bent to form a hook structure. The crack was easily formed on the surface of the component. Therefore, the hook position had to be carefully inspected by the optical microscopy, which was to prevent the emergence of a number of substandard products, to avoid the inflow of substandard products into the next process, to continue processing. For 4Cr13 stainless steel material, the temperature range of the temper brittleness is 550–600 °C. In this study, the temperature of the tempering was lower than that of the temper brittleness. At the same time combination with the microstructure and morphology of the fracture surface, the temper brittleness mode did not occur. After electroless plating, the hydrogen embrittlement usually happened in the steel materials [7]. Hydrogen embrittlement made stainless steel become brittle and fracture due to the introduction and subsequent diffusion of hydrogen into the metal. This was a result of accidental introduction of hydrogen during forming and finishing operations. However, the hydrogen releasing in electroless plating process was inevitable occurrence. After electroless plating, the 4Cr13 component was processed by dehydrogenation. The failure mode of the steel material induced by hydrogen embrittlement was intergranular fracture. However, the intergranular fracture was not found on the fracture surface of the substandard components. It was inferred that the hydrogen embrittlement could be excluded in this study.

4. Conclusions and recommendations

(1) The fracture surface consisted of cleavage terrace with tore edge, dimple and river pattern. The failure mode of 4Cr13 component was the quasi-cleavage fracture.
(2) Compared with the standard sample, the substandard sample exhibited a high hardness, which could cause the strong rigidity, but resulting in the less toughness.
(3) The heat treatment process and other manufacturing processes has a significant effect on the microstructure and mechanical properties of the samples. With increasing the tempering temperature, the hardness of the component was decreased when the quenching temperature was kept stable.

During heat treatment and manufacturing processing for 4Cr13 linkage component, the microcrack was induced sensitivity, finally resulting in the fracture failure of the components under overloading condition. The prevention of 4Cr13 components should control and check the raw material, which could affect the properties of the components. Furthermore, we should control the several special processes, such as the heat treatment processing, annealing, quenching and tempering, and observe the surface of the bending parts after twice bendings, and even plan to test the hardness of the components and other detection technologies. Last, the microcracks should be carefully checked again in each special process. Avoid mechanical damage to the surface, such as scratches and dents, because they can act as crack initiation sites. It was carefully adapted to make installation, operation or maintenance, which was recommended as necessary corrective actions for failure prevention.

References

[1] Zhang LN, Li PN, Tang SW, Tang WB, Zhang S. Mechanical behaviors analysis and Johnson-cook model establish of 4Cr13 Stainless steel. Key Eng Mater 2013;589-590:45–51.
[2] Ouyang JH, Pei YT, Li XD, Lei TC. Effect of tempering temperature on microstructure and sliding wear property of laser quenched 4Cr13 steel. Wear 1994;177(2):203–8.
[3] Hou X-Q, Li Y, Liu C-K, He Y-H. Fracture failure analysis of a 30CrMnSiA steel shaft. J Fail Anal Prev 2012;12(5):485–9.
[4] Sudhakar KV. Metallurgical investigation of a failure in 316L stainless steel orthopaedic implant. Eng Fail Anal 2005;12:249–56.
[5] Pantazopoulos G, Papaefthymiou S. Failure and fracture analysis of austenitic stainless steel marine propeller shaft. J Fail Anal Prev 2015;15(6):762–7.
[6] Cunat PJ. Stainless steel properties for structural automotive applications. In: Metal bulletin international automotive materials conference; 2000.p. 1–10.
[7] Neuharth JJ, Cavalli MN. Investigation of high temperature hydrogen embrittlement of sensitized austenitic stainless steels. Eng Fail Anal 2015;49:49–56.